JOURNAL OF MARINE SCIENCES & ENVIRONMENTAL TECHNOLOGIES
Vol. 2, Issue No.2 (December-2016)

ISSN: 2413-5267

Mineralogy of The Beach Sands Along the Mediterranean Coast from Benghazi to Bin-Jawwad, NE Libya

Osama R. Shaltami[1], Ahmed M. El-Kammar[2], I.H. Arafa[2], and Fares F. Fares[1]

[1]Department of Earth Science, Faculty of Science, University of Benghazi, Benghazi, Libya
[2]Department of Geology, Faculty of Science, Cairo University, Cairo, Egypt

التركيب المعدني لرمال شاطئ البحر على طول ساحل البحر الأبيض المتوسط الممتد من بنغازي حتى بن جواد، شمال شرق ليبيا

أسامة الشالتامي[1]، أحمد الكمار[2]، إ. عرفه[2]، فارس فارس[1]

[1]قسم علوم الأرض، كلية العلوم، جامعة بنغازي، بنغازي، ليبيا
[2]قسم الجيولوجيا، كلية العلوم، جامعة القاهرة، القاهرة، مصر

Abstract

The present work aims to characterize the mineralogy of the beach sands along the Mediterranean Coast from Benghazi to Bin Jawwad, NE Libya. The microscopic and SEM examinations indicate an abundance of carbonates, quartz, feldspars, and evaporites. The detected heavy minerals are zircon, tourmaline, pistachite, hornblende, garnet, monazite, rutile, titanite, augite, biotite, kyanite, chromian spinel, magnetite, ilmenite, and goethite. Carbonate speciation suggests a difference in sediment age; the central and eastern sides consist of younger sediment, while older, reworked, and diagenetically transformed materials dominate in the western section. Three distinct groups of sediments can be recognized according to their mineral composition. The studied beach sands are mineralogically sub-mature sediments depending on the ZTR indices.

Keywords: *Mineralogy; Beach sands; Mediterranean Coast; Libya*.

الملخص

استهدف هذا العمل وصف التركيب المعدني لرمال الشاطئ على طول ساحل البحر الأبيض المتوسط الممتد من بنغازي إلى بن جواد، شمال شرق ليبيا. أشارت الاختبارات والصور المجهرية إلى وجود وفرة من الكربونات، الكوارتز، الفلسبار، والتبخر. المعادن الثقيلة المكتشفة هي الزركون، التورمالين، بيستاكيت، هورنبليندي، العقيق، المونازيت، الروتيل، تيتانيت، أوجيت، البيوتيت، الكيانيت، الكرومين إسبنيل، المغنتيت، إلمنيت، و غوثيت. تشير الكربونات إلى وجود فرق في عمر الرواسب؛ حيث يتكون الجانبان المركزي والشرقي من الرواسب الأصغر سنا، في حين تهيمن المواد الأكبر سنا، والمعاد صياغتها وتحولها في القسم الغربي. ويمكن التعرف على ثلاث مجموعات مختلفة من الرواسب وفقا لتكوينها المعدني. رمال الشاطئ المدروسة هي الرواسب المعدنية ناضجة اعتمادا على مؤشرات ZTR.

الكلمات الدالة: التركيب المعدني، رمال الشاطئ، ساحل البحر الأبيض المتوسط، ليبيا.

1. Introduction

The present work describes the mineralogy of the beach sands along the Mediterranean Coast from Benghazi to Bin Jawwad, NE Libya. The study area is the coastal area of a part of the Sirte Basin (Figure 1). The Sirte Basin ranks the 13th among the world's petroleum provinces,

ISSN: 2413-5267

having proven oil reserves estimated at 43.1 billion barrels of oil equivalent, an amount that constitutes 1.7% of the world's known oil reserves. The basin consists of one dominant total petroleum system, known as the Sirte-Zelten. According to Mresah (1993), the Sirte Basin of Libya is a Mesozoic-Tertiary rift basin comprising a series of horsts and grabens, which were formed as a result of the collapse of an N-S trending arch in the Upper Cretaceous time. The major structural elements of Libya suggest that the Caledonian uplift is trending N-S to NW-SE while the Hercynian structural elements are trending E-W to NE-SW (Figure 2). The collapse of the Hercynian Tibesti-Sirte uplift during the Triassic-Jurassic led to the development of Sirte basin during the Early Cretaceous. The exposed stratigraphic section in the study area consists of sedimentary rocks, ranging in age from Tertiary to Quaternary (Figure 3). The most abundant sedimentary facies are carbonates with lesser amounts of mudrocks, sandstones, and evaporites. Quaternary deposits disseminate around study area along the beach line. They occur as sand dunes, red soil (terra-rossa), conglomerates, calcarenites and sabkha sediments. All sampled stations in the study area are open beaches. There are two beach types; rocky and sandy beaches (e.g., Bin Jawwad and Aqaylah, respectively, Figure 4).

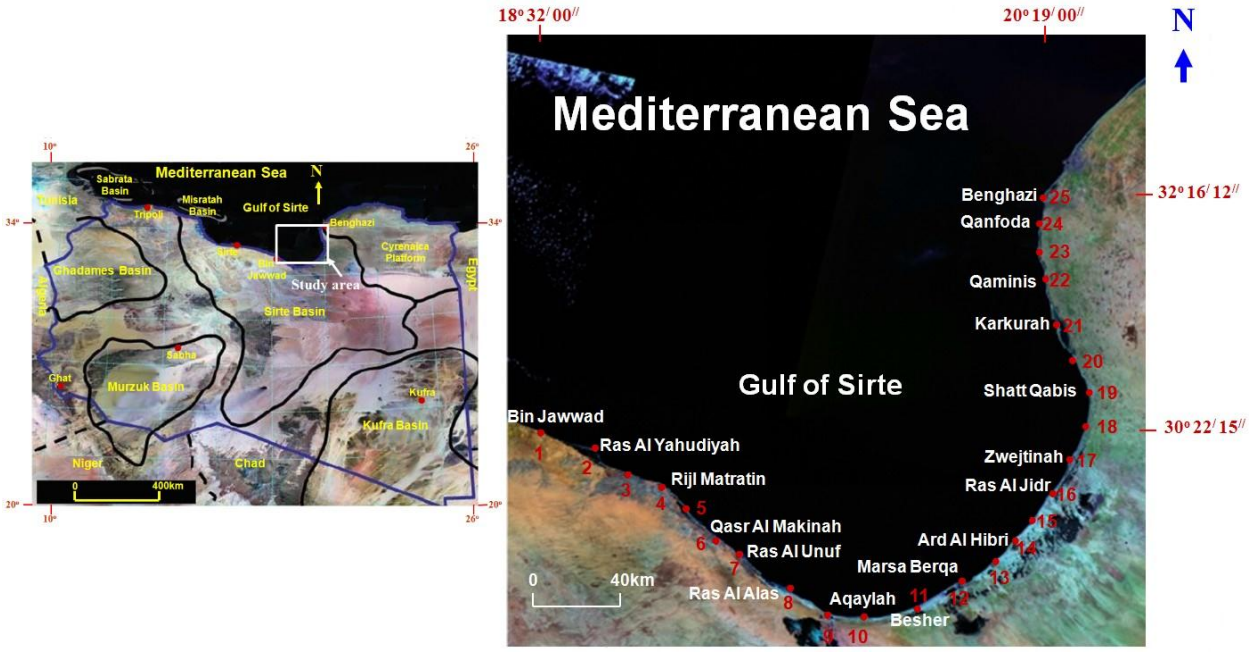

Figure 1. Landsat images showing the location of the study area and the location of the sampled stations

ISSN: 2413-5267

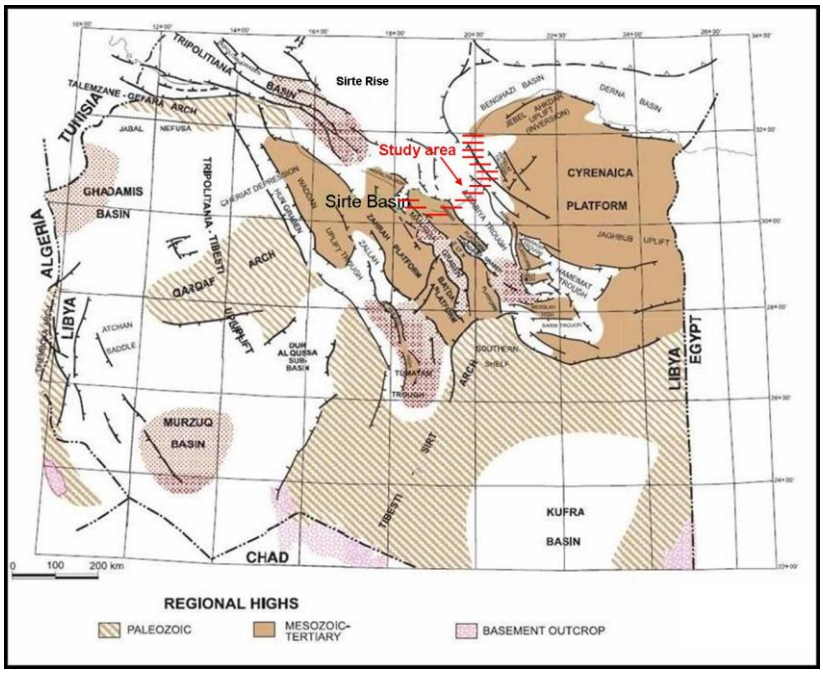

Figure 2. Generalized tectonic map of Libya showing major structural features (modified after Rusk, 2002)

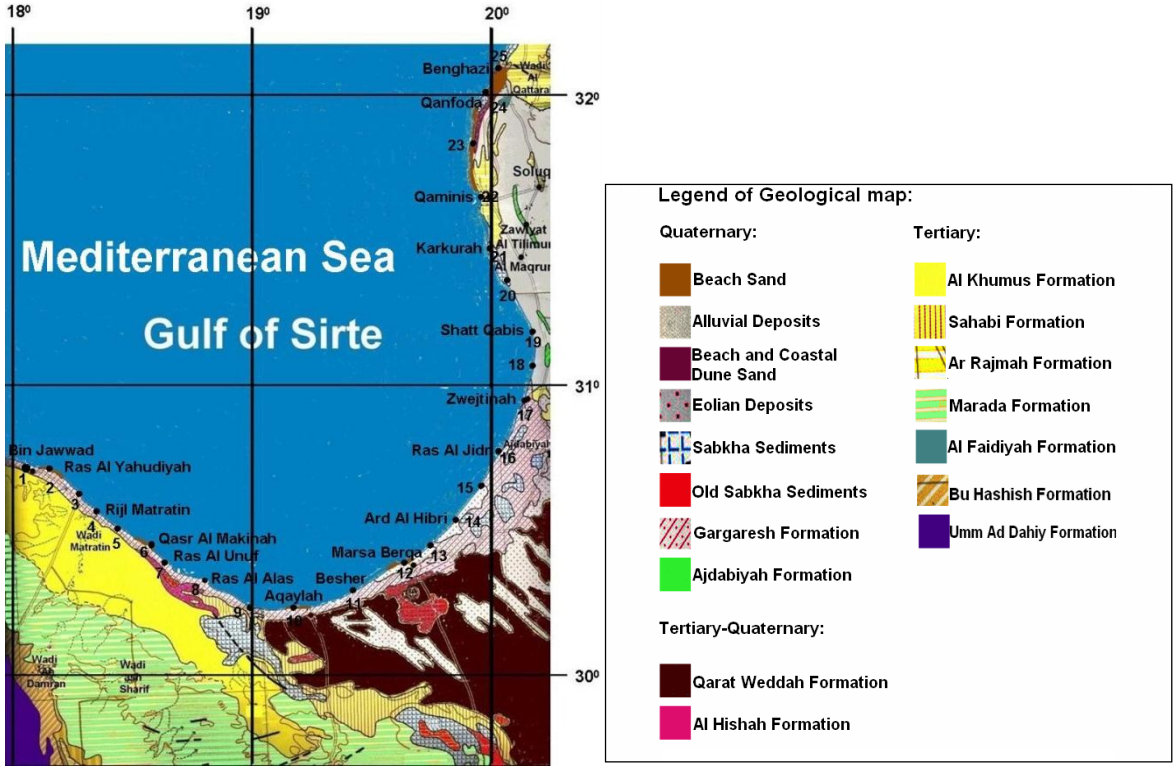

Figure 3. Geological map of the area (scale 1:1,000,000) between Benghazi and Bin Jawwad, NE Libya (modified after Francis and Issawi, 1977; Innocent and Pertusati, 1984; and Mresah, 1998)

ISSN: 2413-5267

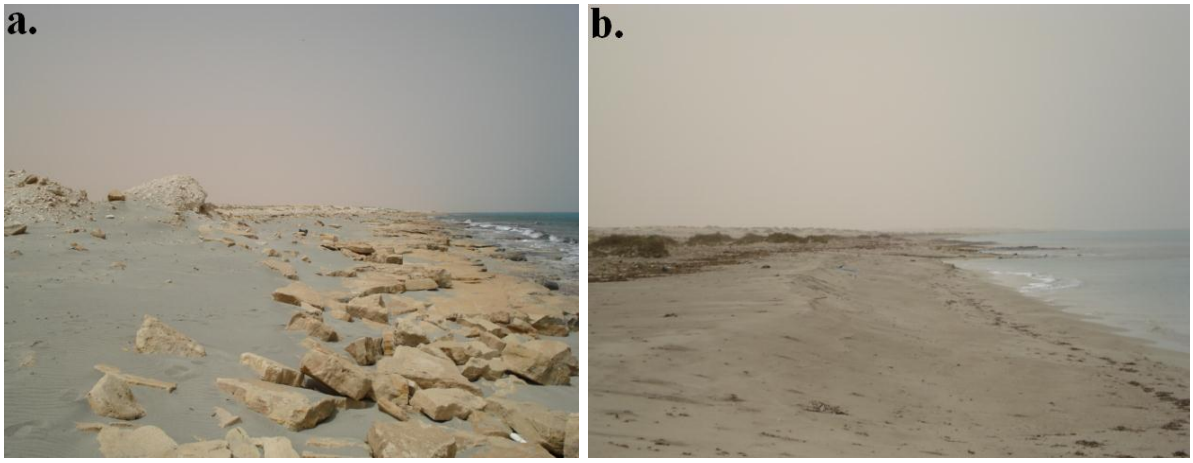

Figure 4. a) Rocky beach (Gargaresh Formation) at station no. 1 (Bin Jawwad) and **b)** Sandy beach at station no.10 (Aqaylah)

As far as the authors are aware, the published data on the beach sands of the study area are insufficient. The studies on the Quaternary are less numerous than those on the Tertiary rocks. Most geological publications on the study area deal with the sedimentary succession with especial attention to petroleum exploration. Limited effort has been given to the beach sands in the study area. Abu El-Ella (2006) and El-Werfalli (2016) studied the mineralogy of beach sands in other parts in Libya.

2. Methodology

Samples were collected from the beach sands along the Mediterranean Coast from Benghazi to Bin Jawwad, NE Libya, from 25 stations (four samples of each station) at sampling interval between 10 and 20 *km*, depending on accessibility to the studied beach. The traverse is parallel to the studied coast. Samples were essentially taken from the surface sands to represent the uppermost 30 *cm* of the beach sands.

The present study is a detailed mineralogical investigation on the very fine and fine sand size fractions (125-63 μm, and 250-125 μm) of the beach sands under consideration. The two size fractions subjected to gravitational heavy mineral separation using bromoform (specific gravity 2.87). The fractions of both the light- and heavy- minerals mounted in Canada balsam for transmitted light microscopy.

Scanning electron microscope with an energy dispersive X-ray attachment (SEM-EDX) used to shed light on the geochemical characteristics of the mineral composition. In spite of the fact that EDX microanalysis extensively used in the present work, its output was not quoted herein because of their standard-less and semi-quantitative nature. The weight or molecular ratios of major oxides used to express the possible changes in composition. The X-

ISSN: 2413-5267

ray powder diffraction of whole samples used to estimate the relative abundance of calcite and aragonite as main partners of the carbonate fraction.

3. Results and Discussions

3.1. Light Minerals

The distribution and morphological properties of light minerals have persuaded many geoscientists to study them with respect to depositional environment and provenance (Trevena and Nash, 1979; Carranza-Edwards *et al.*, 1998; and Margineanu *et al.*, 2014). The studied beach sands are a mixture of carbonate and non-carbonate materials. The microscopic examination and the X-ray powder diffraction of whole-sediment samples indicate an abundance of carbonates, quartz, feldspars and evaporites with other minor minerals. Figures (5 and 6) demonstrate the relative frequency of the light minerals in both the fine and very fine sand fractions.

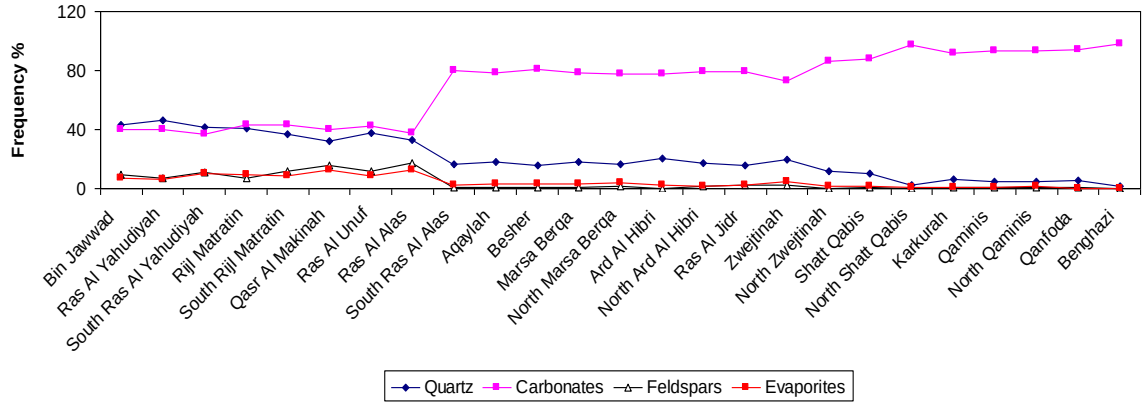

Figure 5. Frequency distribution of the light minerals in the study area (size range: 125-63μm)

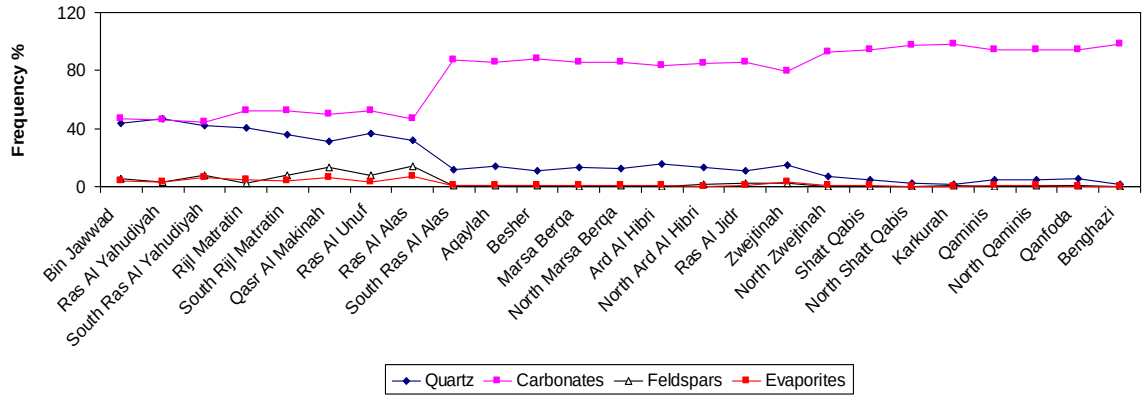

Figure 6. Frequency distribution of the light minerals in the study area (size range: 250-125μm)

ISSN: 2413-5267

3.1.1. Carbonates

According to Schwartz (2005), carbonate beaches have a significant proportion of the sediment fabric of biogenic origin, and carbonate in composition. Carbonate beaches are, therefore, wave deposited accumulations of sediment (sand to boulder in size) deposited on shores where a near shore supply of biogenic debris is available. Carbonate beaches exist in tropical and temperate locations, including some in relatively high latitudes. The main prerequisite for a carbonate beach is a source of carbonate-producing detritus, and a mechanism to erode and/or transport it to the shore. In the studied samples, the recorded carbonate grains include biogenic grains made of aragonite and/or calcite with sporadic dolomite. Calcite is usually colorless and exhibits gleaming interference colors of very high orders (Figure 7). It occurs in form of rounded to subrounded monocrystalline grains (Figure 8) and rounded polycrystalline grains (micrite lumps). Disseminated rhombohedral calcite grains are rarely encountered in the studied samples. The micrite calcite grains are thought to be the product of the mechanical breakdown of the micrite envelopes of recent shell fragments, while rhombohedral calcite grains are thought to be of detrital origin (e.g., Anirudhan and Thiruvikramji, 1991; and Luzar-Oberiter *et al.*, 2008). Biogenic grains are composed of whole shell fragments of macrofauna (mollusks) and microfaunal shells, mostly of foraminifera and algae and other, not clearly classifiable biogenic fragments. The EDX microanalysis of a large number of aragonitic and calcitic specimens suggests that the latter is more capable of hosting more inclusions than the former. These inclusions have different composition but those of barium sulfate and phosphates are abundant (Table 1). The difference in the composition of the inclusions may suggest derivation from various provenances. According to Tucker (2001), the requisite *Mg/Ca* ratios are < 1.2 for low-*Mg* calcite, 1.2 - 5.5 for high-*Mg* calcite, and > 2 for aragonite. Generally, high-*Mg* calcite and aragonite are the predominant mineralogies of organisms in modern seas (*Mg/Ca* ratio=5.2, as quoted by Zankl, 1993). The EDX microanalysis shows that all analyzed grains are low-Mg calcite (*see* Table 1). Pyokari (1997) and El-Werfalli (2016) stated that low-Mg calcite is the most common mineral in the carbonate beach sands. That speciation is rather due to diagenetic transformations of the carbonate material (Preda and Cox, 2005). In the western part of the study area, sands display green color most probably due to algal activity (Figure 9).

ISSN: 2413-5267

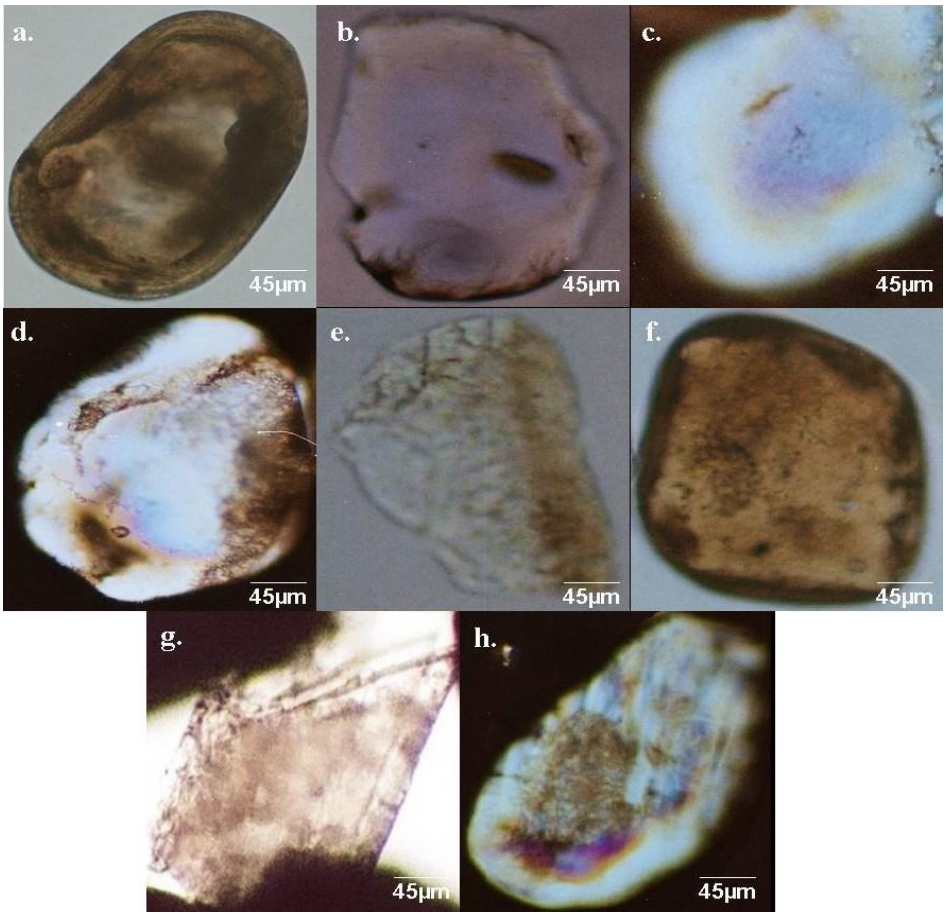

Figure 7. Photomicrographs of light minerals. **a)** well rounded quartz grain, **b)** quartz grain embed tourmaline inclusion, **c)** monocrystalline quartz grain, **d)** polycrystalline quartz grain, **e)** colorless calcite grain, **f)** rhombic dolomite grain, **g)** prismatic gypsum grain and, **h)** microcline grain being turbid due to alteration (size: 125-63μm)

ISSN: 2413-5267

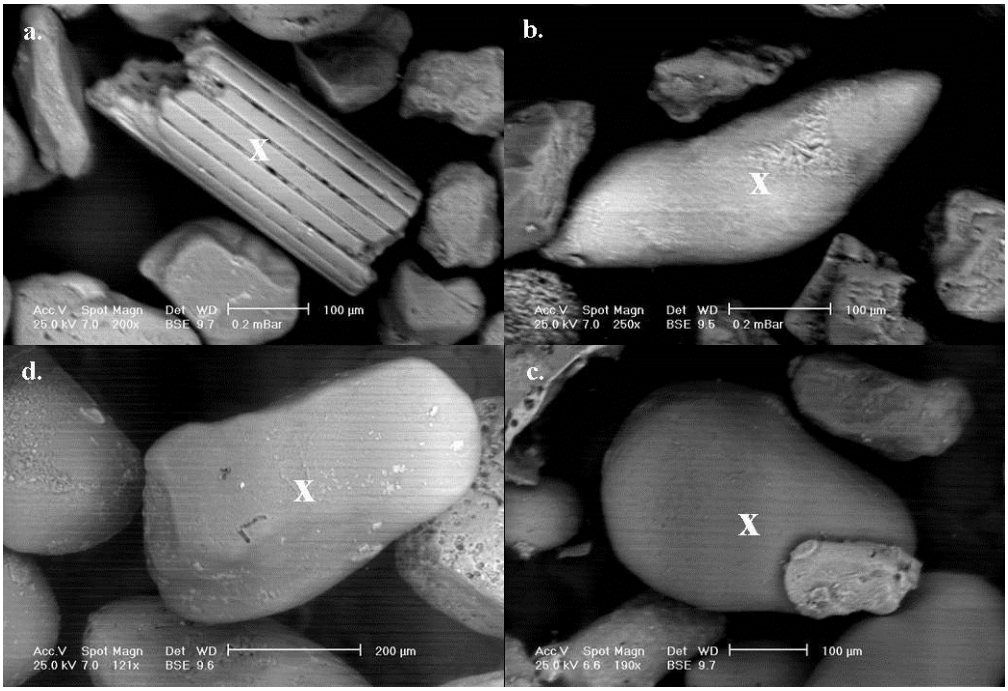

Figure 8. BSE images show calcite shell fragments (a), (b), (c) and (d) from (size: 125-63μm)

Table 1. EDX microanalysis data (relative *wt.%*) of calcite picked from grain size; 125-63μm (carbon and oxygen are excluded)

Elements	Station Name				Average
	Rijl Matratin	Ras Al Unuf	Besher	Benghazi	
Si	7.72	11.45	4.67	<0.5	7.95
Al	1.33	<0.5	<0.5	<0.5	1.33
Fe	2.00	0.36	<0.5	<0.5	1.18
Mg	3.32	0.05	0.05	5.53	2.24
Ca	59.46	88.19	92.50	86.81	81.74
Ba	21.19	<0.5	<0.5	4.46	12.83
P	1.10	<0.5	<0.5	<0.5	1.10
S	3.51	<0.5	1.15	<0.5	2.33
Cl	0.33	<0.5	1.67	3.20	1.73
Mg/Ca	0.06	0.00	0.00	0.06	0.03

ISSN: 2413-5267

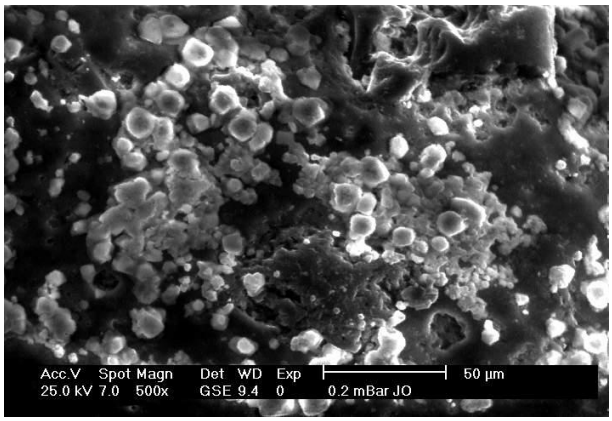

Figure 9. BSE image of algae from Bin Jawwad (size: 125-63μm)

The XRD analysis (Table 2) shows that in the central and eastern sides of the studied beach, aragonite dominates over calcite. This feature is possibly related to a number of regional characteristics such as biological production. In the western section calcite dominants over aragonite. That speciation is rather due to diagenetic transformations of the carbonate material. In agreement with Preda and Cox (2005), carbonate speciation suggests a difference in sediment age; the central and eastern sides consist of younger sediment, while older, reworked, and diagenetically transformed materials dominate in the western section.

Table 2. Calcite/aragonite ratio on basis of XRD analyses

	Location	calcite/aragonite
West	Bin Jawwad	1.73
	South Ras Al Yahudiyah	1.46
	Ras Al Unuf	1.50
Center	South Ras Al Alas	0.75
	North Marsa Berqa	0.83
	North Ard Al Hibri	0.57
	Shatt Qabis	0.72
East	North Shatt Qabis	0.74
	Qanfoda	0.59

3.1.2. Quartz

In the studied beach sands, quartz is commonly colorless and contains inclusions, namely, tourmaline (*see* Figure 7), rutile, and apatite. It is mostly monocrystalline with uniform and undulatory extinction. However, some samples contain polycrystalline quartz grains. It is important to notice that abrasion during transportation may affect the relative abundance of the polycrystalline and undulatory quartz because they destroy preferentially relative to non-undulatory monocrystals (Lewis, 1984). According to Cherian *et al.*, (2004), the reduced

ISSN: 2413-5267

percentage of the polycrystalline quartz is probably due to dilution by a fresh supply of monocrystalline quartz. Moreover, the polycrystalline quartz grains may disintegrate during the course of transportation from source. The detected quartz grains vary from very angular to well-rounded with relative preponderance of the former type. According to Shine (2006), the rounded and well-rounded quartz grains owe their shape largely to a longer distance of transportation and/or the multi-cycle origin of clastic sediments. On the other hand, moderate to high degree of sphericity of the quartz grains are an indication of derivation from crystalline and older sedimentary rocks exposed in regions far from the basin of deposition (Rahman *et al*., 2004). The presence of dust rims in most quartz grains as an indicator for sediment recycling has long been recognized (e.g., Dickinson and Milliken, 1995). Some quartz grains show cracks, which could be either due to inheritance from source material or due to long transportation distance.

3.1.3. Feldspars

In the present study, microcline and members of plagioclase series are common feldspars. Microcline is mainly colorless rectangular, in few cases, the microcline grains are altered and turbid (*see* Figure 7). Plagioclase feldspars occur mainly as fresh grains.

3.1.4. Evaporites

In the studied sands, the detected evaporites are gypsum and halite (Figure 10). Gypsum occurs as prismatic, nodular, tabular and lenticular grains. The fabric and texture of gypsum grains suggest their authigenic crystals. Halite crystallizes together with gypsum. It is frequently recorded some zircon and Ti-minerals as tiny inclusions.

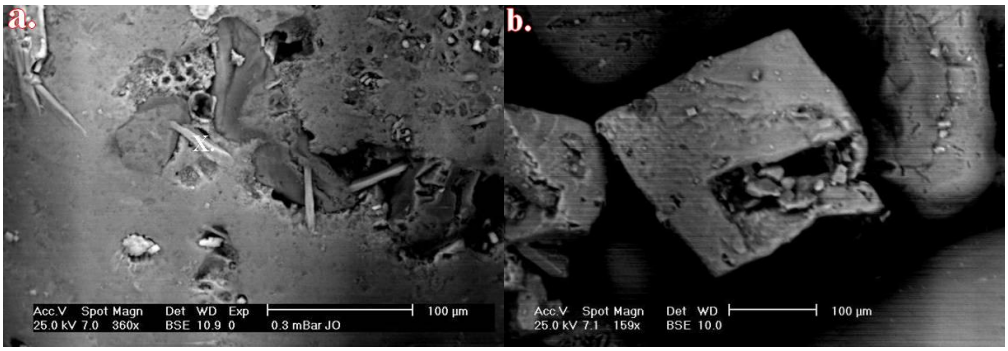

Figure 10. BSE images showing. **a)** prismatic crystals of gypsum on Mg- silicate matrix where halite crystals and tiny zircon inclusions are recorded, and **b)** well cubic halite grain (size: 125-63**µm**)

3.2. Heavy minerals

The microscopic investigation documents that some minerals such as kyanite and titanite occur exclusively in the western part of the study area. Hornblende, pistachite and garnet

ISSN: 2413-5267

disappear in the eastern part, whereas zircon, tourmaline, monazite, augite, biotite and rutile exist in the whole area under consideration.

3.2.1. Zircon

Zircon represents the most abundant heavy mineral among the non-opaques. Microscopic observations of zircon enabled the recognition of different shapes of zircon, such as; the oval with zoned structure, elongated, elliptical, outgrown, overgrown, rounded and broken (Figure 11). It generally contains different amounts of inclusions as well as vacuoles or bubbles. Well-developed fractures crisscrossed the zircon grains might probably be due to their sustained transportation by waves and currents (e.g., Angusamy and Rajamanickam, 2000). It is important to notice that the outgrown and broken zircon grains are copiously present in the very fine sand fraction. According to Angusamy *et al.,* (2004), the prolific presence of broken zircon in the beach sand of southern coast of Tamil Nadu, east coast of India, indicate rigorous energy conditions by waves, due to repeated swash and backwash and by littoral currents. The same authors added that outgrown zircon might be due to the longer stay of sediments in the depositional environment. Some of the examined zircon displays evident metamictized nature (Figure 12). Based on the semi-quantitative EDX microanalysis data (Table 3), there are two types of zircon in the studied samples; the first type is uranium and thorium enriched whereas the second is yttrium and heavy rare earth elements enriched. This suggests the possibility of zircon from different provenances.

ISSN: 2413-5267

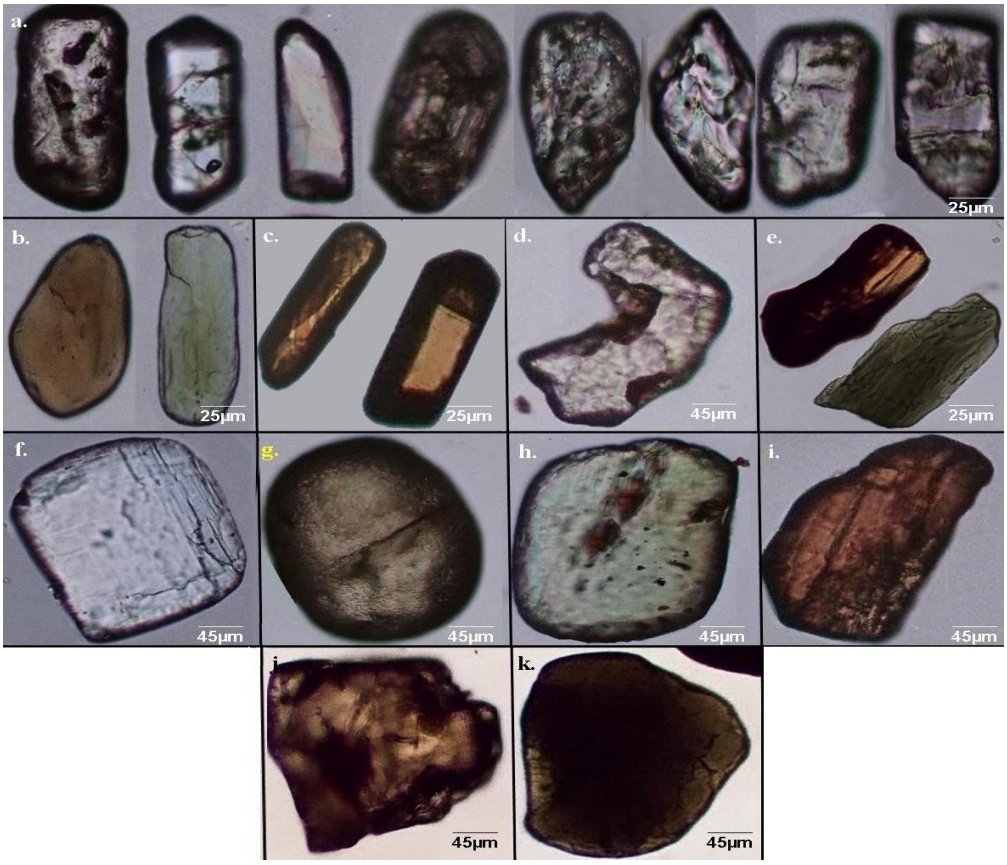

Figure 11. Photomicrographs of; **a)** Oval shaped with zoned structure zircon grains displaying elongated, elliptical, outgrown, overgrown, rounded, and broken forms. **b)** Green and brown tourmaline grains, **c)** Yellowish brown and deep reddish brown rutile grains. **d)** Colorless garnet grain. **e)** Green and brown hornblende grains. **f)** Colorless kyanite grain showing cleavage. **g)** Well rounded monazite grain. **h)** Rounded turbid pistachite grain. **i)** Reddish brown titanite grain. **j)** Yellowish brown augite grain. **k)** Green biotite green (size: 125-63μm).

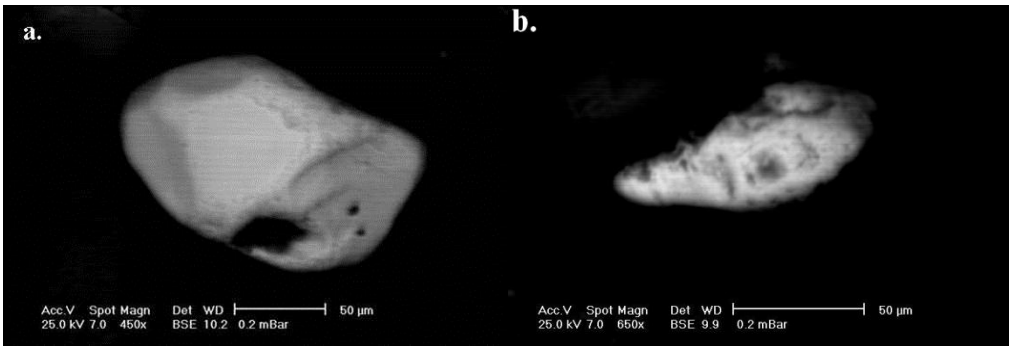

Figure 11. BSE images of; **a)** metamictized rectangular zircon, and **b)** highly dissolved zircon grain (size: 125-63μm)

ISSN: 2413-5267

Table 3. EDX microanalysis data (relative *wt. %*) of zircon picked from grain size; 125-63µm (carbon and oxygen are excluded)

Elements	Location		Average
	Ras Al Unuf	Ard Al Hibri	
Si	21.22	33.90	27.56
Al	0.79	0.90	0.85
Fe	1.27	0.38	0.83
Ca	8.73	0.27	4.50
Y	4.43	<0.5	4.43
Zr	59.82	61.27	60.55
Hf	1.83	1.15	1.49
Th	<0.5	1.02	1.02
U	<0.5	1.10	1.10
Yb	1.88	<0.5	1.88

3.2.2. Tourmaline

It is the second common non-opaque mineral. Zircon is present in higher frequencies in very fine-grained sediments, whilst tourmaline dominates in fine-grained sands. This observation coincides with that quoted by Sallun and Suguio (2008) in their study on Quaternary deposits from Sao Paulo State, Brazil. This can be attributed to differences in the hardiness of these minerals. Most of the tourmaline grains are surrounded to well-rounded but sometimes prismatic in shape. The authors believe that the occurrence of a rounded to well-rounded tourmaline variety suggests recycling from the older sedimentary precursor and the high frequency of tourmaline in the studied sediments may indicate derivation from metasomatized-rich tourmaline source rock. The majority of the encountered grains are zoneless. Zoning, if present, is visible as a faint change in color intensity. Tourmaline grains display a wide range of colors and pleochroism represented by pale yellowish brown, pale green and pink.

3.2.3. Hornblende

The frequency of hornblende is lower in the size fraction 250-125μm than the finer size fraction 125-63μm. It is commonly brown, light green and bluish green to dark green (*see* Figure 11). It displays diagnostic perfect cleavage that appears imperfect in some cases, depending on the optical orientation of the mounted grains. They are mostly prismatic in shape but occasionally sub-rounded.

3.2.4. Pistachite

It is only detected in the grain size; 125-63µm. This result is similar to the study of the beach sands along the eastern side of the Gulf of Suez, Egypt as quoted by El-Kammar *et al.*, (2007). According to Anfuso *et al.*, (1999), in the coastal sand between Sanlucar de

ISSN: 2413-5267

Barrameda and Rota, Cadiz, southwest Iberian Peninsula, pistachite accumulates in the finer fraction. In the present study, pistachite is commonly pale yellowish green in color; sometimes it is turbid due to alteration with weak pleochroism and high birefringence as a diagnostic character.

3.2.5. Garnet

According to Anfuso *et al.*, (1999) garnet is more abundant in the coarsest fractions. In the studied samples, it is slightly abundant in the size fraction 250-125μm than in the size fraction 125-63µm. The encountered garnet grains are angular to subangular but occasionally sub-rounded with characteristic conchoidal fracture (Figure 13). The most common grains are colorless (*see* Figure 11) but few pinkish grains occur also. In some cases, garnet contains opaque and quartz inclusions. The EDX microanalysis shows that detected garnet is mostly of almandite variety (Table 4).

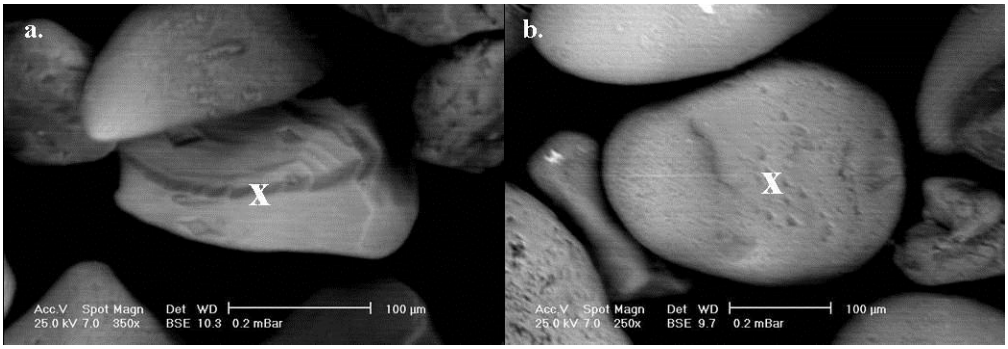

Figure 13. BSE images show, **a)** sub-angular garnet grain, and **b)** rounded garnet grain (size: 125-63μm)

Table 4. Semi-quantitative EDX microanalysis data (*wt. %*) of garnet picked from grain size; 125-63μm (carbon and oxygen are excluded)

Oxides	Location		Average
	Ras Al Unuf	Besher	
SiO_2	40.34	41.47	40.91
TiO_2	0.40	0.88	0.64
Al_2O_3	20.24	30.53	25.39
Fe_2O_3	30.66	20.52	25.59
MnO	2.37	0.00	1.19
MgO	3.96	3.17	3.57
CaO	2.03	3.43	2.73

ISSN: 2413-5267

3.2.6. Monazite

It is pale yellow in color with high relief and very weak birefringence (*see* Fig. 11). It occurs as rounded grains of spherical and ellipsoid shapes, sometimes with strongly pitted surface.

3.2.7. Rutile

It either occurs as subangular grains or rounded grains (Fig. 14) with a relative preponderance of the former. The yellowish-brown and deep reddish brown colors characterize the encountered rutile (*see* Fig. 12). It is a well-known fact that rutile can contain highly charged elements (V, Cr, Fe, Al, Nb, Sn, Sb, Ta, W) up to the %-level (Smith and Perseil, 1997; Zack, *et al.*, 2004). The EDX microanalysis shows that the studied rutile is a good accumulator of chromium (Table 5). The rutile composition is not the same in the studied sediments, suggesting derivation from various provenances.

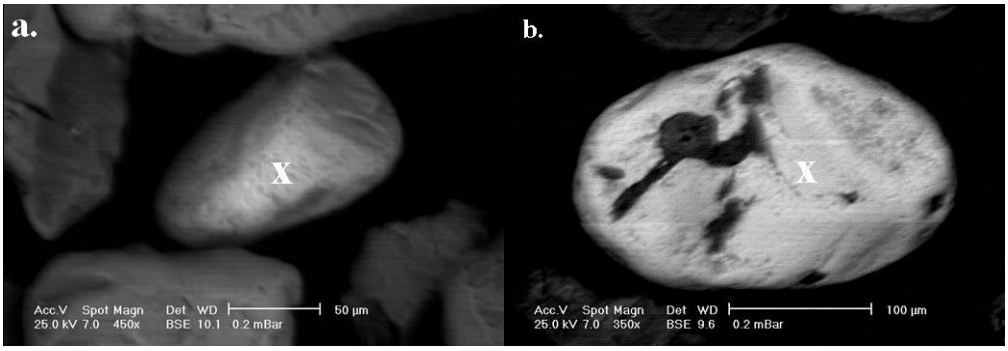

Figure 14. BSE images show, **a)** subangular rutile grain, and **b)** rounded rutile grain (size: 125-63*µm*)

Table 5. Standard-less EDX microanalysis data (*wt.%*) of rutile picked from grain size; 125-63*µm* (carbon and oxygen are excluded)

Oxides	Location		Average
	Marsa Berqa	Besher	
SiO_2	7.52	6.69	7.11
TiO_2	90.26	62.68	76.47
Al_2O_3	1.50	1.25	1.38
Fe_2O_3	0.72	27.13	13.93
MnO	0.00	1.73	0.87
CaO	0.00	0.28	0.14
SO_3	0.00	0.24	0.12
Cr_2O_3	0.00	0.00	0.00

ISSN: 2413-5267

3.2.7. Titanite

The reddish brown titanite is the only detected type (*see* Figure 11). It is commonly prismatic to sub-rounded grains in shape, occasionally displaying imperfect cleavage.

3.2.8. Augite

Its frequency is slightly lower in the size fraction 250-125*μm* than in the finer size fraction 125-63μm. It has yellowish brown color (*see* Figure 11) and exhibits perfect cleavage.

3.2.9. Biotite

It dominates in the 250-125*μm* size fraction. It belongs to the green variety of biotite (*see* Figure 11) and seems to be fresh with diagnostic bright yellowish peripheries. Fine inclusions of opaque minerals are sometimes frequent.

3.2.10. Kyanite

It is only detected in the grain size 125-63*μm*. It occurs as colorless short prismatic sub-rounded grains with marked right-angled cleavage (*see* Figure 11).

3.2.11. Chromian spinel

Its recognition was through the SEM examination (Figure 15) and not microscopically. The EDX microanalysis (Table 6) shows that Al_2O_3:MgO:Fe_2O_3 is 2:1:1, where Cr_2O_3>Al_2O_3 and the *Cr/(Cr+Al)* ratio about 0.52. This indicates that the spinels represent the *Cr-Al* trend (e.g., Oszczypko and Salata, 2005).

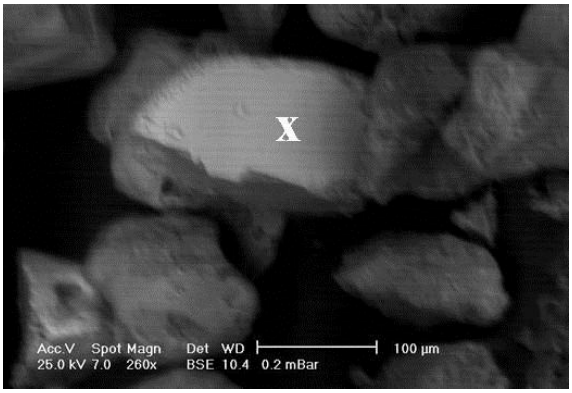

Figure 15. BSE image and EDX microanalysis data (*wt.%*, excluding *C* and O_2) of chromian spinel grain (size: 125-63*μm*)

ISSN: 2413-5267

Table 6. EDX microanalysis data (*wt.%*, excluding *C* and O_2) of chromian spinel grain (size: 125-63μm)

Oxides	Location
	Ras Al Unuf
SiO_2	7.08
TiO_2	0.38
Al_2O_3	30.51
MgO	15.21
Fe_2O_3	13.23
CaO	0.54
SO_3	0.13
Cr_2O_3	32.93

3.2.12. Opaque minerals

The SEM examination indicates that the detected opaque minerals are mainly magnetite, ilmenite, and goethite (Figure 16). According to Mohapatra *et al.*, (2016), ilmenite is commonly present in the very fine sand fraction.

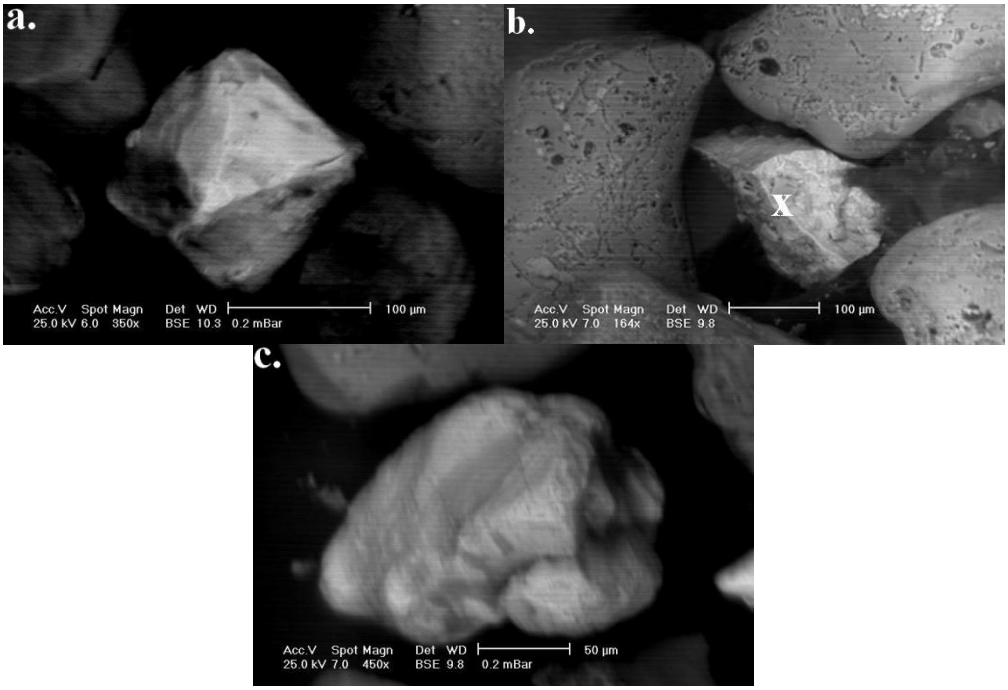

Figure 16. BSE images of, **a)** octahedral magnetite grain, **b)** broken ilmenite grain, and **c)** irregular goethite grain(size: 125-63μm)

ISSN: 2413-5267

3.3. Sediments Type

Mixes of carbonate and clastic sediments, which are commonly encountered in the Recent coastal sediments, require careful analysis if they are to be correctly interpreted (Carter, 1982). Various methods can identify and quantify the mixing of carbonate and clastic sediments. Mount (1985) pointed out that carbonate sediments incorporate more than 10% terrigenous constituents considered to be of a mixed carbonate-clastic character. On the other hand, varied levels of $CaCO_3$ content propose transition region between the terrigenous and carbonate provinces, commonly ranging from 25 to 75% (Hernandez Arana *et al.*, 2005). In agreement with Gomez-Pujol *et al.*, (2013), the authors believe that cluster analysis can classify the sampled stations (Figure 17) as follows:

3.3.1. Province One (from Bin Jawwad to Ras Al Alas)

The sediments of this province contain mixtures of clastics related to different sedimentary rocks of limestones, evaporites, sandstones and mudrocks, along with green sediments. Mineralogically, in this province quartz and carbonates are present in roughly equal abundances, with feldspars and evaporites contents in the range of 7 to 17% and 6 to 13%, respectively. Medium to high concentration of heavy minerals characterizes also this province. The detected heavy minerals are zircon, tourmaline, pistachite, hornblende, garnet, monazite, rutile, titanite, augite, biotite, and kyanite.

3.3.2. Province Two (from South Ras Al Alas to Shatt Qabis)

The sediments of this province consist of a mixture of clastics derived mostly from sandstones and limestones. Mineralogically, in this province carbonates dominate over quartz, with minor feldspars and evaporites in the range of 0.24 - 3%, and 1 - 5%, respectively, with a complete absence of titanite and kyanite.

3.3.3. Province Three (from North Shatt Qabis to Benghazi)

Mineralogically, the clastics of this province are carbonate-dominated, with subordinate quartz but very poor in feldspars and evaporites. The heavy minerals in this province are extremely rare. Zircon, tourmaline, monazite, augite, biotite and rutile are the only detected heavy minerals.

Based on the difference in minerals concentration among the three provinces, and considering the geology of the surrounding areas, the authors believe that the studied beach sands in provinces one and two were derived from the sea accumulation (carbonates and evaporates), surrounding carbonate rocks (carbonates), terra-rossa soil and sandstones (quartz, feldspars and heavy minerals). In province three, the sands are derived from the sea accumulation (carbonates and evaporates) and surrounding carbonate rocks (carbonates). The heavy minerals and some light minerals (quartz and feldspars) originated from the aeolian

ISSN: 2413-5267

sands related to the widely distributed igneous and metamorphic rocks in many parts of Libya such as Jabal Al Tibisti, Jabal Al Haruj Al Swad, etc.

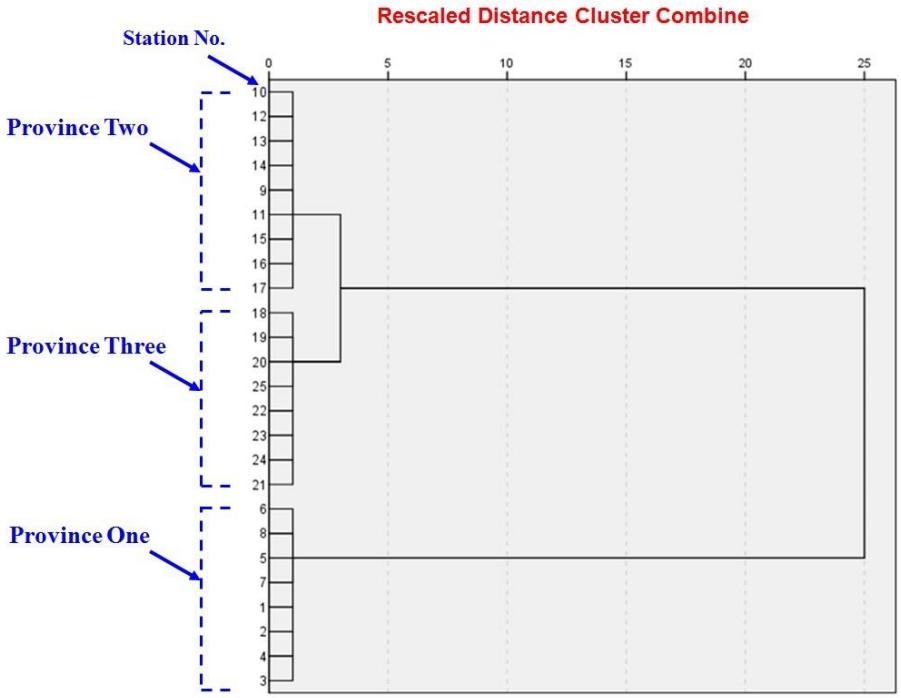

Figure 17. Dendrogram from cluster analysis (Ward method) of the sampling stations

3.4. Maturity

The abundance of the ultrastable heavy minerals, e.g., zircon, rutile, and tourmaline (ZRT) indicate mature sediments (Carver, 1971). The presence of high percentage of metastable minerals, e.g., garnet, kyanite and staurolite indicate immature sediments (Dar, 1998). According to Hubert (1962), the zircon-tourmaline-rutile (ZRT) index is calculated as; ZTR index = ((zircon+ tourmaline + rutile)/ ∑ non-opaque heavy minerals)*100. According to Madukwe *et al.*, (2014), ZTR < 50 % implies immature sediments, 50 < ZTR < 75 % implies typically sub-mature sediments and ZTR >75 % indicates mineralogically mature sediments. In the present study, the ZTR index varies from 52.52 to 71.14 %, suggesting a sub-mature nature of the studied beach sand sediments.

4. Conclusions

The present study provides genuine data on the "very fine" and "fine" sand size fractions (125-63μm and 250-125μm) of the beach sands along the Mediterranean Coast from Benghazi to Bin Jawwad, Northeast Libya. These sediments represent a mixture of carbonate and non-carbonate materials at different quotients. The detected light minerals are calcite, aragonite,

ISSN: 2413-5267

quartz, feldspars, and evaporites, whereas the recorded heavy minerals are zircon, tourmaline, pistachite, hornblende, garnet, monazite, rutile, titanite, augite, biotite, kyanite, chromian spinel, magnetite, ilmenite, and goethite. The heavy minerals in the eastern side are extremely rare, while medium to high concentration of heavy minerals characterizes the sands of the western and central parts. The XRD analysis shows that aragonite dominates over calcite, in the central and eastern sides of the studied beach, whereas calcite dominants over aragonite in the western side, suggesting a difference in sediment age. The central and eastern sides consist of younger sediment, while older, reworked and diagenetically transformed material dominates in the western section. The cluster analysis extracted three distinct groups of sediments. The ZTR index suggests that the studied beach sands are mineralogically sub-mature sediments.

References

Abu El-Ella N.A. (2006). *Sedimentological, mineralogical and geomorphological studies on the Quaternary sediments of the coastal area, W. Tripoli, Libya*. Ph.D Thesis, Cairo University, Cairo, Egypt.

Anfuso G., Achab M., Cultrone G., and Lopez-Aguayo F. (1999). Utility of heavy minerals distribution and granulometric analyses in the study of coastal dynamics: Application to the littoral between Sanlucar de Barrameda and Rota (Cadiz, southwest Iberian Peninsula). *Boletin Instituto Espanol DE Oceanografia*, 15(1-4): 243-250.

Angusamy N., Loveson V.J., and Rajamanickam G.V. (2004). Zircon and ilmenite from the beach placers of southern coast of Tamil Nadu, east coast of India. *Indian Journal of Marine Sciences*, 33(2): 138-149.

Angusamy N., and Rajamanickam G.V. (2000). Distribution of heavy minerals along the beach from Mandapam to Kanyakumari, Tamil Nadu. *Journal of the Geological Society of India*, 56: 99-211.

Anirudhan S., and Thiruvikramji K.P. (1991). Petrography of light detrital grains: a case study from Bharathapuzha, Kerala, India. *Journal of Earth Science*, 18: 27–32.

Anketell J.M. (1996). Structural history of the Sirt Basin and its relationships to the Sabratah Basin and Cyrenaican Platform, Northern Libya. In M.J. Salem, A.S. El-Hawat, and A.M. Sbeta, eds., *Geology of the Sirt Basin*. Amsterdam, Elsevier, 3: 57–88.

Carranza-Edwards A., Bocanegra-Garcia G., Rosales-Hoz L., and Galan L.D. (1998). Beach sands from Baja California Peninsula, Mexico. *Sedimentary Geology*, 119(3-4): 263-274.

Carter R.W.G. (1982). Some problems associated with the analysis and interpretation of mixed carbonate and quartz beach sands, illustrated by examples from North-West Ireland. *Sedimentary Geology*, 33: 35-56.

Carver R.E. (1971). *Procedures in sedimentary petrology*. John-Wiley Inc., New York, USA.

ISSN: 2413-5267

Cherian A., Chandrasekar N., and Rajamanickam V. (2004). Light minerals of beach sediments from Southern Tamilnadu, south east coast of India. *Oceanologia*, 46 (2): 233-252.

Dickinson W.W., and Milliken K.L. (1995). The diagenetic role of brittle deformation in compaction and pressure solution, Etjo Sandstone, Namibia. *Journal of Geology*, 103: 339-347.

El-Kammar A.M., Arafa I.H., and Shaltami O.R. (2007). Mineral composition and environmental geochemistry of the beach sediments along the eastern side of the Gulf of Suez, Egypt. *Journal of African Earth Sciences*, 49: 103–114.

El-Werfalli B.A. (2016). *Mineralogy and geochemistry of the beach sands along the coast between Al Kuwifia and Tolmeita, NE Libya*. MSc Thesis, Benghazi University, Benghazi, Libya.

Francis M., and Issawi B. (1977). *Geological map of Libya, 1:250,000 sheet: Soluq NI 34-2*. Explanatory Booklet, Ind. Res. Centre, Tripoli, Libya.

Gomez-Pujol L., Roig-Munar F.X., Fornos J.J., Balaguer P., and Mateu J. (2013). Provenance-related characteristics of beach sediments around the island of Menorca, Balearic Islands (western Mediterranean). *Geo-Marine Letters*, 33:195–208.

Hernandez Arana H.A., Attrill M.J., Hartley R., and Bouchot G.G. (2005). Transitional carbonate-terrigenous shelf sub-environments inferred from textural characteristics of surficial sediments in the Southern Gulf of Mexico. *Continental Shelf Research*, 25(15): 1836–1852.

Hubert A. (1962). The geology of part of southwestern Nigeria. *Geological Survey of Nigeria Bulletin*; 3: 87.

Innocent F., and Pertusati P. (1984). *Geological map of Libya; 1:250,000 sheet: Al Aqaylah NH 34-5*. Explanatory Booklet, Ind. Res. Centre, Tarabulus, Libya.

Lewis D.W. (1984). *Practical Sedimentology*. Hutchison Ross publ. Co., Stroudsburg, USA.

Luzar-Oberiter B., Pavlakovic S.M., Crnjakovic M., and Babic L. (2008). Variable sources of beach sands of north Adriatic islands: examples from Rab and Susak. *Geologia Croatica*, 61(2-3): 379–384.

Madukwe H.Y., Akinyemi S.A., Adebayo O.F., Ojo A.O., Aturamu A.O., and Afolagboye L.O. (2014). Geochemical and petrographic studies of Lokoja sandstone: Implications on source area weathering, provenance, and tectonic setting. *International Journal of Scientific and Technology Research*, 3: 21-32.

Margineanu R.M., Blebea-Apostu A.M., Celarel A., Gomoiu C.M., Costea C., Dumitras D., Ion A., and Duliu, O.G. (2014). Radiometric, SEM and XRD investigation of the Chituc black sands, southern Danube Delta, Romania. *Journal of Environmental Radioactivity*, 138: 72-79.

Mohapatra S., Behera P., and Senapaty A. (2016). Heavy mineral potentiality in part of Chhatrapur Beach, Odisha, India. *Special Publication in Geology*, 14: 122-128.

ISSN: 2413-5267

Mount J.F. (1985). Mixed siliciclastic and carbonate sediments: a proposed first- order textural and compositional classification. *Sedimentology*, 32(3): 435–442.

Mresah M.H. (1993). Facies patterns and stratal geometries: clues to the nature of the platform margin during the Paleocene, northeast Sirte Basin, Libya. *Sedimentary Geology*, 84(1-4): 149-167.

Mresah M.H. (1998). The massive dolomitization of platformal and basinal sequences: proposed models from the Paleocene, Northeast Sirt Basin, Libya. *Sedimentary Geology*, 116(3-4): 199-226.

Oszczypko N., and Salata D. (2005). Provenance analyses of the Late Cretaceous –Palaeocene deposits of the Magura Basin (Polish Western Carpathians) – evidence from a study of the heavy minerals. *Acta Geologica Polonica*, 55(3): 237-267.

Preda M., and Cox M.E. (2005). Chemical and mineralogical composition of marine sediments, and relation to their source and transport, Gulf of Carpentaria, Northern Australia. *Journal of Marine Systems*, 53: 169-186.

Pyokari M. (1997). The provenance of beach sediments on Rhodes, southeastern Greece, indicated by sediment texture, composition and roundness. *Geomorphology*, 18: 315-332.

Rahman M.A., Alam M.S., and Shine F.M.M. (2004). Roundness and Sphericity of Calstic Sediments of Apical Part of the Tista Fan in Panchagarh District, Bangladesh. *Rajshahi University Studies, Part-B.*

Rusk D.C. (2002). Libya: Petroleum potential of the underexplored basin centers—a twenty-first-century challenge, in Downey, M.W.. Threet, J. C. and Morgan, W. A. eds., Petroleum provinces of the twenty-first century: *AAPG Memoir*, 74: 429–452.

Sallun A.E.M., and Suguio K. (2008). Sedimentological characterization of the Quaternary deposits in the region between Marília and Presidente Prudente, Sao Paulo State, Brazil. *REM: Revista Escola de Minas, Ouro Preto*, 61(3): 343-356.

Schwartz M.L. (2005). *Carbonate Sandy Beaches*. Encyclopedia of Coastal Science; 2.

Selley R.C. (1978). *Ancient Sedimentary Environments*. 2nd edit., Richard Clay (The Chaucer Press) Ltd, Bungay, Suffolk, England.

Shine F.M.M. (2006). Shape Analysis of Detrital Quartz Grains and its Environment of Deposition in Holocene Sediments along the Karotoya River, Bogra, Bangladesh. *Journal of Geo-Environment*, 6: 54-63.

Smith D.C., and Perseil E.A. (1997). Sb-rich rutile in the manganese concentrations at St. Marcel-Praborna, Aosta Valley, Italy: petrology and crystal-chemistry. *Mineralogical Magazine*, 61: 655- 669.

Trevena A.S., and Nash, W.P. (1979). Chemistry and provenance of detrital plagioclase. *Geology*, 7: 475-478.

ISSN: 2413-5267

Tucker M.E. (2001). *Sedimentary petrology: an introduction to the origin of sedimentary rocks*. Oxford: Blackwell, UK.

Zack T., von Eynatten H., and Kronz A. (2004). Rutile geochemistry and its potential use in uantitative provenance studies. *Sedimentary Geology*, 171: 37-58.

Zankl H. (1993). The origin of High-Mg-Calcite microbialites in cryptic habitats of Caribbean coral reefs—Their dependence on light and turbulence. *Facies*, 29: 55-59.